THE JOURNAL OF PHYSICAL CHEMISTRY C

Article

pubs.acs.org/JPCC

Structural Dynamics at Monolayer–Liquid Interfaces Probed by 2D IR Spectroscopy

Daniel E. Rosenfeld, Jun Nishida, Chang Yan, S. K. Karthick Kumar, Amr Tamimi, and Michael D. Fayer*

Department of Chemistry, Stanford University, Stanford, California 94305, United States

ABSTRACT: Monolayers functionalized with tricarbonyl-1,10-phenanthroline rhenium chloride ($RePhen(CO)_3Cl$) are studied in the presence of a variety of polar organic solvents (chloroform, tetrahydrofuran, dimethylformamide, acetonitrile), hexadecane, and water. The headgroup, $RePhen(CO)_3Cl$, is soluble in the bulk polar organic solvents but not in hexadecane or water. The surface structural dynamics are studied using IR absorption, ultrafast two-dimensional infrared (2D IR) vibrational echoes, and heterodyne-detected transient gratings (HDTG). The headgroup is also studied in the bulk solvents. Immersion in solvent changes the environment of the surface bound $RePhen(CO)_3Cl$ as shown by a solvent-dependent symmetric CO stretch absorption frequency and line shape. The 2D IR spectroscopy is sensitive to spectral diffusion, which reports on the structural time dependence. In the absence of solvent (bare surface), the spectral diffusion takes place on a 37 ± 4 ps time scale, whereas in the presence of THF, MeCN, or $CHCl_3$ it occurs on the 25 ± 6 ps time scale. However, in DMF, the spectral diffusion time constant is 15 ± 3 ps. In hexadecane the spectral diffusion slows to 77 ± 15 ps, slower than the bare surface. In D_2O, the monolayer CO stretch is split into two bands, indicating distinct local structures, and the spectral diffusion of main band is again slower than the bare surface. HDTG spectroscopy is used to investigate the vibrational lifetime dynamics.

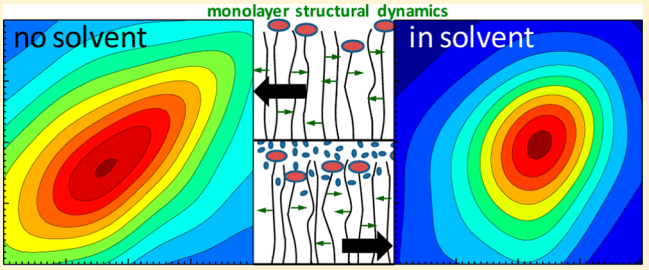

I. INTRODUCTION

Thin films and molecular monolayers are of fundamental interest and importance in science and technology. Molecular monolayers are used to control surface properties and reactions in a variety of scientific and technological fields including microelectrical-mechanical systems,[1] chemical sensors,[2] and microelectronics.[3,4] Functionalized molecular monolayers are also an important class of systems for performing molecular heterogeneous catalysis.[5−8] In many of the practical uses of molecular monolayers, functionalized surfaces come into contact with different chemical environments, e.g., solvents. Understanding how functionalized surface properties are different from the same chemical species in bulk and how surface properties including dynamics of the molecular surface layer change with exposure to different chemical conditions is important for building a more complete understanding of these important physical and chemical systems.

To study the impact of solvent on the structure and dynamics of molecular monolayers, we extend our previous work on $RePhen(CO)_3Cl$-functionalized monolayers.[9,10] Previous studies of these monolayers using ultrafast two-dimensional infrared vibrational echo (2D IR) spectroscopy have shown they have ∼40 ps time scale structural dynamics in the absence of solvent (bare).[10] These thin films are well suited for the study of the impact of solvent on the structure and dynamics of monolayers for several reasons. The monolayers can be studied optically because they are deposited on SiO_2-on-CaF_2 substrates that are transparent in both the IR and visible spectral regions. The symmetric CO stretch of the $RePhen(CO)_3Cl$ headgroup is spectrally isolated and in a relatively background free portion of the mid-infrared for many solvents. Also, the chromophore density of the monolayers can be made very high, with most alkane chains functionalized with a vibrationally active probe molecule. The $RePhen(CO)_3Cl$ headgroup is an excellent mid-infrared probe and is sensitive to its environment.[9] At the surface concentrations studied here there is no vibrational excitation transfer, which can obscure ultrafast spectroscopic measurements of structural dynamics.[10] By measuring the complete IR line shape (homogeneous broadening, inhomogeneous broadening, and spectral diffusion) with linear IR and 2D IR spectroscopy in the presence of solvents, we can obtain information on how the solvents change the structure and dynamics of molecular monolayers.

2D IR spectroscopy has proven valuable for studying dynamics of molecular systems in the bulk. It has permitted the elucidation of the molecular dynamics in water,[11−15] confined water, and concentrated aqueous salt solutions[16] as well as the dynamics of solute–solvent complex formation[17,18] and the structure and dynamics of proteins and polypeptides.[19−29] Transforming 2D IR into a technique for surface study recently has been successful via both the direct third-order vibrational echo method and fourth-order time-resolved SFG method.[30−35] The 2D IR method has made possible the measurement of spectral diffusion of molecules bound to the

Received: November 10, 2012
Revised: December 23, 2012
Published: December 27, 2012

 © 2012 American Chemical Society dx.doi.org/10.1021/jp311144b | J. Phys. Chem. C 2013, 117, 1409−1420

surface for substrates that produce no bulk signal,[9,10] while the fourth-order method is intrinsically surface selective and has been useful for studying systems with large bulk contributions to the third-order response functions.[32−35] Because the monolayers investigated here are on transparent, nonabsorptive substrates, the third-order echo based technique is preferred as it is more sensitive and interpretable by standard procedures.

Many studies have examined the impact of surfaces (solid, hydrophobic, monolayers, air, etc.) on water or the structure of monolayer air interfaces.[32,36−40] However, how solvents change the structure and dynamics of surface functionalized monolayers has not been a topic studied in depth. Although changes in water structure at hydrophobic surfaces have been investigated for many years, changes in the hydrophobic surface upon hydration have not been studied to any extent. Yet, changes to the hydrophobic thin film upon wetting are also of importance technologically.[41,42] Often the thin film is deposited on a substrate to change the tribological properties of the surface or to protect the underlying material.[1,41,43] Changes to the structure of the monolayer can change the properties and performance of the monolayer. Here, we immerse the functionalized monolayers in polar organic solvents, hexadecane, and water. Each liquid has an impact on surface dynamics, and results show that water changes the structure and dynamics of the monolayer, despite its hydrophobicity.

$RePhen(CO)_3Cl$ and related Re metal complexes are photocatalysts for the reduction of CO_2 to CO.[44−47] More generally, supported metal complexes are an important class of systems for performing heterogeneous catalysis with immobilized homogeneous catalysts.[8] The $RePhen(CO)_3Cl$ system is particularly interesting as a tool for investigating solvent effects in immobilized homogeneous catalyst systems as there are strong solvent effects in the homogeneous system. In the catalytic cycle for this class of molecules, the solvent acts as a ligand at various times during the reaction cycle.[48] Therefore, the properties of the solvent can determine the catalytic enhancement or even which product is favored (H_2 or CO).[46,49] For example, with DMF as a solvent, CO is produced by the catalyst, and with THF as a solvent, H_2 is produced.[46] Furthermore, when DMF and MeCN are used as solvents, the CO_2 insertion reaction to displace hydrogen from the complex is fastest.[49] Although electronic or chemical effects could be dominant contributors to the solvent effects on the catalytic activity due to the role of the solvent as a coordinating ligand, it is interesting that we observe that the solvents all modify the spectral diffusion (structural dynamics) of the symmetric CO stretch of the metal complex, as measured through 2D IR spectroscopy. Spectral diffusion reports on the sampling of the ground state potential energy surface by the metal complex, which also in part determines the kinetics of the catalytic cycle. We observe that the changes to the dynamics of the immobilized complex with solvent are different from those of the complex in the same bulk solvents.

One of the notable properties of heterogeneous catalysts is that the choice of the solvent for the catalytic reaction is not limited by the solubility of the immobilized headgroup. Thus, it may be possible that heterogenized homogeneous catalysts provide new combinations of catalysts and liquids which have distinct chemical activities. From this point of view, it is useful to understand how the catalytic headgroup behaves in a liquid in which it cannot dissolve. Our results show that the surface dynamics in solvents that do not dissolve the headgroup in the bulk liquids tend to be slower than in the headgroup soluble polar organic liquids.

II. EXPERIMENTAL METHODS

A. Synthesis of Functionalized Monolayers on Silica-on-Calcium Fluoride. Silica-on-calcium fluoride (SiO_2-on-CaF_2) windows were prepared from 3 mm thick CaF_2 windows using with plasma-enhanced chemical vapor deposition. The CaF_2 windows were exposed to a low-frequency plasma of nitrous oxide (N_2O) and silane (SiH_4) gas at a temperature of 350 °C and a pressure of 650 mTorr.

Subsequently, the SiO_2-on-CaF_2 substrates were alkylated using bromine functionalized trichlorosilane. The SiO_2-on-CaF_2 substrates were immersed in 10 mL of bicyclohexyl (Aldrich, 99%). 10 μL of 11-bromoundecyltrichlorosilane (ACBR GmBH; 95%) was injected into the bicyclohexyl. After 1 h the wafers were removed and sonicated in toluene (Sigma-Aldrich) for 30 s and ethanol (Sigma-Aldrich) for 30 s to remove the remnant reactants.

The alkane deposition was followed by S_N2 substitution of the terminal Br by azide (N_3). A saturated sodium azide (NaN_3; Sigma-Aldrich) solution in DMF (Sigma-Aldrich) was prepared. The wafers with alkyl layers prepared above were immersed in the NaN_3 saturated solution for 24 h. The wafers were then sonicated in DMF, water, and ethanol, each for 3 min. The success of the deposition and substitution was verified by FT-IR absorption spectroscopy of the azide stretch at about 2100 cm^{-1}.

The azide group on the end of the alkyl chain was used to immobilize *fac*-Re(phenC≡CH)$(CO)_3Cl$ (synthesized by standard methods) through a copper-catalyzed azide−alkyne cycloaddition (CuAAC). 0.3 mM *fac*-Re(phenC≡CH)(CO) was dissolved in 5 mL of a 2:1 dimethyl sulfoxide (DMSO):-water binary mixture along with 0.3 mM $CuSO_4$ and 0.3 mM TTMA (triethyl 2,2′,2″-(4,4′,4″-(nitrilotris(methylene))tris-(1*H*-1,2,3-triazole-4,1-diyl))triacetate). The substrates with terminal azide group were immersed in the reactant solution, and 1.7 mL of 10 mM ascorbic acid aqueous solution was added to the reaction vessel. The solutions and head space were then purged with N_2, and the beakers were sealed and left for 2 days at room temperature. The substrates were removed and sonicated in 2:1 DMSO:water mixture for 10 min and rinsed with DMSO, water, and ethanol.

FT-IR absorption spectroscopy was performed on the functionalized substrates (two different samples were used for the nonlinear optical study), and the absorption band peak at 2022 cm^{-1} (symmetric stretching mode of carbonyl; 0.8−1.0 mOD for the surfaces studied here) confirmed the success of the cycloaddition reaction. Because of the harsh solvents used throughout the course of study, the initial absorption slowly decayed throughout the long nonlinear optical experiments. Despite some loss of material, the IR line shape was not impacted once the solvent was removed. Previous results indicate no concentration or sample dependence in the dynamics of the monolayers.[10] Therefore, it is acceptable to compare the results obtained from the two different surface functionalized samples immersed in different solvents over the course of several months.

B. Ultrafast Two-Dimensional Infrared Vibrational Echo Spectroscopy. 2D IR vibrational echo spectroscopy is a method for examining sub-picoseconds to picoseconds dynamics of molecules in condensed phases. Recently the technique has also been used to probe functionalized

surfaces.[9,10] Since the experimental and theoretical details have been described fully elsewhere,[10,15,50] only a brief description of the method is given here. Mid-infrared laser pulses are generated using a regeneratively amplified Ti:sapphire laser system which pumps an optical parametric amplifier (OPA). The OPA is pumped by 640 μJ 800 nm laser pulses with 15 nm of bandwidth. 5 μJ mid-infrared pulses centered at 2025 cm^{-1} with a 90 cm^{-1} bandwidth and a 170 fs transform limited duration are generated.

The mid-infrared laser pulse is beam split into three excitation pulses and a local oscillator pulse. The three excitation beams are combined at the sample in the BOXCARS geometry which results in a phase-matched nonlinear optical signal, the vibrational echo, propagating in a unique direction. The echo pulse is combined with the local oscillator pulse and passed through a monochromator used as a spectrograph. The frequency-dependent interference between the local oscillator and nonlinear optical signal is monitored through the use of a 32-element HgCdTe array. The time delays between the three incident pulses are controlled using precision mechanical delay lines.

For the study of bulk samples by 2D IR spectroscopy, an acousto-optic modulator pulse shaping systems with a collinear excitation geometry for pulses 1 and 2 was used.[51,52] The third pulse, which is crossed in the sample with the path of pulses 1 and 2, also serves as the local oscillator. The AOM-based pulse shaping 2D IR methodology helps with the suppression of scatter,[53] reduces data acquisition time,[52,54] and permits phase-locked data acquisition.[51] The collinear geometry, however, fixes the intensity of the local oscillator to that of the third excitation pulse, resulting in decreased sensitivity.[52,55] The pulse shaping experimental setup was used for the higher optical density (>10 mOD for carbonyls) bulk solution samples, while the standard delay line vibrational echo method, which is superior for the ultralow optical density (<1 mOD), was used for the surface samples. The two methods have been shown to produce identical results.[51]

Regardless of the excitation scheme, the three incident laser pulses interact with the vibrational resonance (the CO stretching mode) to generate a vibrational echo. The direct observable in 2D IR is the interferogram obtained by scanning the interval between the first two pulses, τ, while the period between the second and third pulse, T_w (the population period), is held fixed. During the population period, the vibrational frequency evolves because of structural dynamics. After T_w, the third pulse gives rise to the emitted vibrational echo pulse. The frequencies measured by the monochromator are denoted ω_m (the vertical axis in the 2D spectra). At each ω_m, a time-domain interferogram is generated as τ is scanned. By Fourier transforming the interferograms acquired at each ω_m, a spectrum with respect to ω_τ (the horizontal axis in the 2D spectrum) is obtained. A 2D IR spectrum is generated by plotting the ω_τ spectrum for each ω_m. The ω_τ axis is the initial excitation frequency of molecular vibrations, and the ω_m axis is the vibrational echo emission frequency of the same vibrations after a time T_w.

A series of 2D IR spectra recorded at different T_w's are obtained. The time-dependent information is contained in the change of shape of the 2D spectrum with T_w. Analyzing the 2D line shape yields quantitative measurements of the homogeneous broadening, spectral diffusion, and inhomogeneous broadening of the vibration under study. Homogeneous broadening is caused by extremely rapid fluctuations that produce a motionally narrowed (Lorentzian) contribution to the absorption line shape. In contrast, inhomogeneous broadening originates from the vibrational frequency shift due to different more slowly evolving molecular environments. Spectral diffusion is the time-dependent stochastic fluctuations in vibrational frequency induced by microscopic changes in the structural environment that causes sampling of the inhomogeneous environments. It is characterized by the frequency–frequency correlation function (FFCF). The 2D IR spectra acquired as a function of T_w are analyzed using the center-line-slope (CLS) method, which extracts the normalized FFCF.[56,57] Using this method, the series of 2D IR spectra are transformed into a single decay curve. The decay of the CLS gives the spectral diffusion decay time(s). The deviation of the CLS value at T_w = 0 ps from 1 gives the extent of homogeneous broadening. By combining the CLS and the linear IR absorption spectrum, the full FFCF, including the spectral diffusion and the homogeneous component, is obtained.

The FFCF is described with a multiexponential model

$$C_1(t) = \langle \delta\omega_{1,0}(\tau_1)\delta\omega_{1,0}(0)\rangle = \sum_i \Delta_i^2 \exp(-t/\tau_i) \quad (1)$$

where the Δ_i are the frequency fluctuation amplitudes (standard deviations) of each component, and the τ_i are their associated time constants. For a component of the FFCF where $\Delta\tau < 1$, the component is motionally narrowed and Δ and τ cannot be determined separately. The motionally narrowed homogeneous contribution to the absorption spectrum has a pure dephasing line width $\Gamma^* = 1/\pi T_2^*$, where $T_2^* = 1/\Delta^2\tau$ is the pure dephasing time. The homogeneous line width is usually dominated by pure dephasing, but the observed homogeneous dephasing time, T_2, also has contributions from the vibrational lifetime and orientational relaxation:

$$\frac{1}{T_2} = \frac{1}{T_2^*} + \frac{1}{2T_1} + \frac{1}{3T_{or}} \quad (2)$$

where T_2^*, T_1, and T_{or} are the pure dephasing time, vibrational lifetime, and orientational relaxation time, respectively. The total homogeneous line width is $\Gamma = 1/\pi T_2$.

C. Heterodyne-Detected Transient Grating (HDTG) Spectroscopy. Transient grating spectroscopy can measure the dynamical observables, vibrational lifetime, and orientational relaxation, typically probed in transient absorption (pump–probe) spectroscopy with greater sensitivity.[10,58–60] Pump–probe experiments are not feasible for surface samples due to low optical density (0.5–1 mOD). In transient grating spectroscopy, the first two pulses are crossed in the sample simultaneously, making a sinusoidal optical interference pattern. The interference pattern generates a transient diffraction grating, where the modulation in optical properties is caused by the varying amounts of molecular absorption in the peaks and nulls of the interference pattern. After a waiting time (T_w), a third beam hits the sample and is diffracted by the grating pattern made by the two time coincident excitation pulses. As the waiting time gets longer, molecules in the vibrational excited state relax to the ground state and, as a result, the grating pattern fades out. Molecules can also undergo orientational relaxation, which changes the anisotropy of the diffraction grating and therefore the diffraction efficiency. The fading of the grating is observed as a decrease in the electric field amplitude of diffracted beam. Therefore, in the absence of orientational relaxation, the decay time constant of the

dx.doi.org/10.1021/jp311144b | J. Phys. Chem. C 2013, 117, 1409–1420

diffracted amplitude with respect to the waiting time T_w corresponds to the population relaxation (lifetime) of the vibrational mode.

For an arbitrary value of T_w, the transient grating signal can range from being in phase with the local oscillator (constructive interference) to out of phase with the local oscillator (destructive interference). To circumvent this difficulty, the timing between the first two pulses (τ) was scanned from −5 fs to +5 fs in 1 fs steps. Since the duration of the infrared pulses are ∼170 fs, the overlap in time of the two excitation pulses changes negligibly, but the phase of the emitted signal oscillates as τ is scanned. The amplitude of the oscillation is determined by nonlinear fitting to a sinusoidal function. The amplitude of a number of scans is averaged to determine the grating modulation. Measuring the grating modulation as a function of T_w yields the time dependence of the vibrational population relaxation and anisotropy decay. The same geometry used in vibrational echo experiments is employed in the HDTG spectroscopy. The diffracted signal pulse propagates in the same direction as the phase matched direction of the vibrational echo signal and is combined with the same local oscillator.

III. RESULTS AND DISCUSSION

A. Infrared Absorption Spectroscopy. FT-IR absorption spectroscopy was performed on monolayers functionalized with RePhen(CO)$_3$Cl in contact with various liquids and on samples of the RePhen(CO)$_3$Cl headgroup dissolved in bulk solutions. RePhen(CO)$_3$Cl attached by a triazole linker to an undecane chain was also studied when dissolved in chloroform ($CHCl_3$). In bulk solution IR absorption spectra were measured in acetonitrile (MeCN), acetone, dichloromethane (DCM), $CHCl_3$, DMF, and THF. For the functionalized surfaces, IR absorption spectra were measured in contact with MeCN, $CHCl_3$, DMF, THF, hexadecane, D_2O, and also in air (bare, no solvent). The spectra for both bulk (A) and surface (B) samples in the CO symmetric stretching region (∼2025 cm^{-1}) are shown in Figure 1. Regardless of whether the RePhen-(CO)$_3$Cl molecule is in bulk solution or immobilized on the surface, the solvent has a significant effect on the vibrational frequency and line width. Both DCM and $CHCl_3$ shift the symmetric CO stretch frequency to the blue (higher frequency) relative to acetone, whereas DMF, THF, and MeCN shift it to the red (lower frequency) of acetone. The directions of the shifts in bulk solutions match those on the surface where DMF, THF, and MeCN all shift the vibrational frequency to the red of the bare sample, and $CHCl_3$ and D_2O shift the frequency to the blue relative to the bare sample. There is also a strong effect on the line width (full width at half-maximum, fwhm) of the absorption. In the bulk, the line widths in the polar organic solvents studied range from 5.9 cm^{-1} (THF) to 7.8 cm^{-1} ($CHCl_3$) (see Table 1). In comparing the spectra from the monolayers to the bulk solutions, there is the question of whether the triazole and alkane chain themselves, which are used to immobilize the headgroup to the surface, affect the properties of the headgroup. To evaluate this possibility, the headgroup was "clicked" (CuAAC reaction) to undecane azide with azide−alkyne cycloaddition described above to give the headgroup with triazole and alkane chain. Comparison of the headgroup only IR spectrum in bulk $CHCl_3$ with the headgroup with triazole and alkane chain in bulk $CHCl_3$ (labeled $CHCl_3$* in Figure 1) shows that the additional organic moieties have basically no effect on the absorption spectrum (see Figure 1 and Table 1) as the peak positions and line widths are identical within experimental error. The identity of the two spectra indicates that the alkane chain and triazole have no impact on the CO absorption spectrum while the solvent does influence the spectra.

On the surface, contact with the solvents (except for D_2O) cause the symmetric carbonyl mode of the Re complex

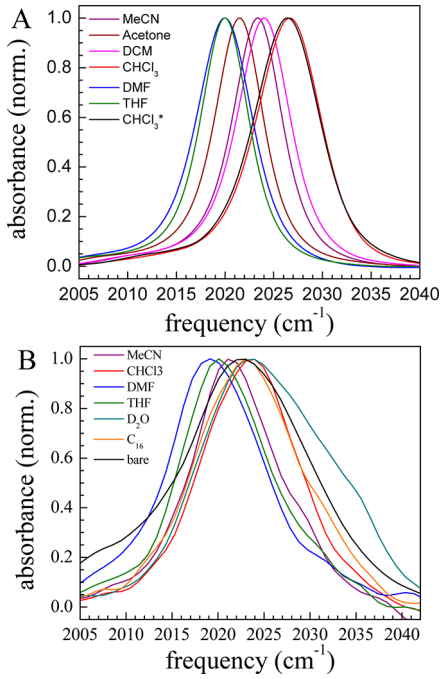

Figure 1. (A) IR absorption spectra for RePhen(CO)$_3$Cl in various polar organic solvents: acetonitrile (purple), acetone (maroon), DCM (magenta), chloroform (red), DMF (blue), THF(green). (B) IR absorption spectra for RePhen(CO)$_3$Cl functionalized molecular monolayers on SiO_2-on-CaF_2 substrates. The peak shifts are smaller but similar in nature to those in the bulk. $CHCl_3$, hexadecane (C_{16}; orange), and D_2O (cyan) shift the line center to the blue whereas other solvents caused a red shift in frequency.

Table 1. IR Absorption Peak Position and Full Width at Half-Maximum for the Symmetric CO Stretch of RePhen(CO)$_3$Cl in Bulk Solution (Headgroup Only, Except for $CHCl_3$ Where an Undecane Chain Has Been Clicked to the Headgroup To Model Chain Effects) and Immobilized through a Triazole Linker on Alkylated SiO_2-on-CaF_2 Substrates[a]

solvent	ν_{bulk} (cm^{-1})	$\Delta\nu_{bulk}$ (cm^{-1})	$\varepsilon_{int,bulk}$ (10^5 M^{-1} cm^{-2})	$\nu_{surface}$ (cm^{-1})	$\Delta\nu_{surface}$ (cm^{-1})
none				2022.6	16.2
D_2O				2023.5	13.4, 10.2
hexadecane				2023.0	13.3
MeCN	2023.4	6.1	2.54	2021.3	10.7
DMF	2020.0	6.8	2.98	2019.4	10.9
THF	2020.0	5.9	2.51	2020.0	11.1
$CHCl_3$	2026.8	7.8	3.19	2023.7	12.3
$CHCl_3$[b]	2026.8	8.0		2023.7	12.3
DCM	2024.0	6.5	3.22		
acetone	2021.5	6.0	2.74		

[a] ν = peak frequency in wave numbers, $\Delta\nu$ = full width at half-maximum in wavenumbers, and ε_{int} = integrated (in wavenumbers) molar decadic extinction coefficient. [b] Chromophore has triazole and alkane chain attached.

dx.doi.org/10.1021/jp311144b | J. Phys. Chem. C 2013, 117, 1409−1420

absorption line width to be narrowed from 16.2 cm^{-1} for the bare surface to under 13.3 cm^{-1} (hexadecane; $CHCl_3$, 12.3 cm^{-1}; THF, 11.1 cm^{-1}; DMF, 10.9 cm^{-1}; MeCN, 10.7 cm^{-1}) (see Table 1). Because of the very low absorbencies of the surface molecules, background subtraction is not perfect, and the spectra have some mild distortion.

Under D_2O the symmetric stretch displays a distinct shoulder on the blue side of the line that is not due to imperfect background subtraction. Figure 2 shows that the spectrum of the Re complex under D_2O is well fit by two Gaussians, one centered at 2023.5 cm^{-1} and one at 2034 cm^{-1}, with 13.5 and 10.2 cm^{-1} line widths, respectively. The appearance of the shoulder demonstrates that there are two distinct $RePhen(CO)_3Cl$ environments in the monolayer. For example, there could be $RePhen(CO)_3Cl$ headgroups that are preferentially exposed to D_2O while a majority of the headgroups are more buried in the monolayer. Regardless of the details of the water/surface interaction, it is clear that D_2O has a strong effect on the monolayer structure, despite the monolayer being hydrophobic. The peak height of the symmetric CO stretch of the second population of $RePhen(CO)_3Cl$ headgroups has some sample variation. Other experiments documented in the literature have shown effects of water on hydrophobic surfaces[41,42] and changes to the water at hydrophobic surfaces.[40,61] The clear changes to the IR spectrum illustrate that the $RePhen(CO)_3Cl$ is reporting on the impact of D_2O on the monolayer.

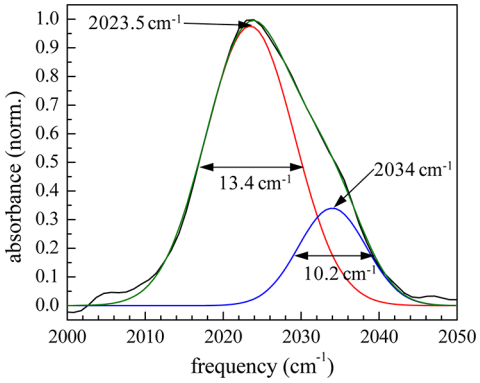

Figure 2. IR absorption spectrum for the $RePhen(CO)_3Cl$ functionalized monolayer immersed in D_2O. The CO stretch is split into two bands. The total spectrum is well fit by the sum of two Gaussians.

The FT-IR spectra show that there is no correlation between vibrational frequency (or line width) and the dielectric constant of the solvent in the bulk. The lack of correlation suggests that chemical effects, rather than local field or dielectric medium effects, are responsible for the shifts in frequency in the bulk. The role of solvent chemical effects on the headgroup infrared absorption is further supported by the strong dependence of the integrated extinction coefficient on solvent (see Table 1). Analysis based on a local field model for the transition dipole explains little of the variance.[62] There is also a strong correlation between the vibrational frequencies in the bulk and on the surface immersed in the same solvent, suggesting that there are also significant headgroup−solvent interactions on the surface. The line widths are strongly correlated, indicating that the heterogeneity due to the solvent−headgroup interaction contributes significantly to the surface line width. The bare surface line width shrinks when the surface is immersed in solvents, indicating that the presence of solvent changes the microstructure or dynamics of the surface. Changes to the line shape can occur either through the effects of motional narrowing or changes in the extent of inhomogeneous broadening. 2D IR spectroscopy enables the direct measurement of these two types of changes to the line broadening processes.

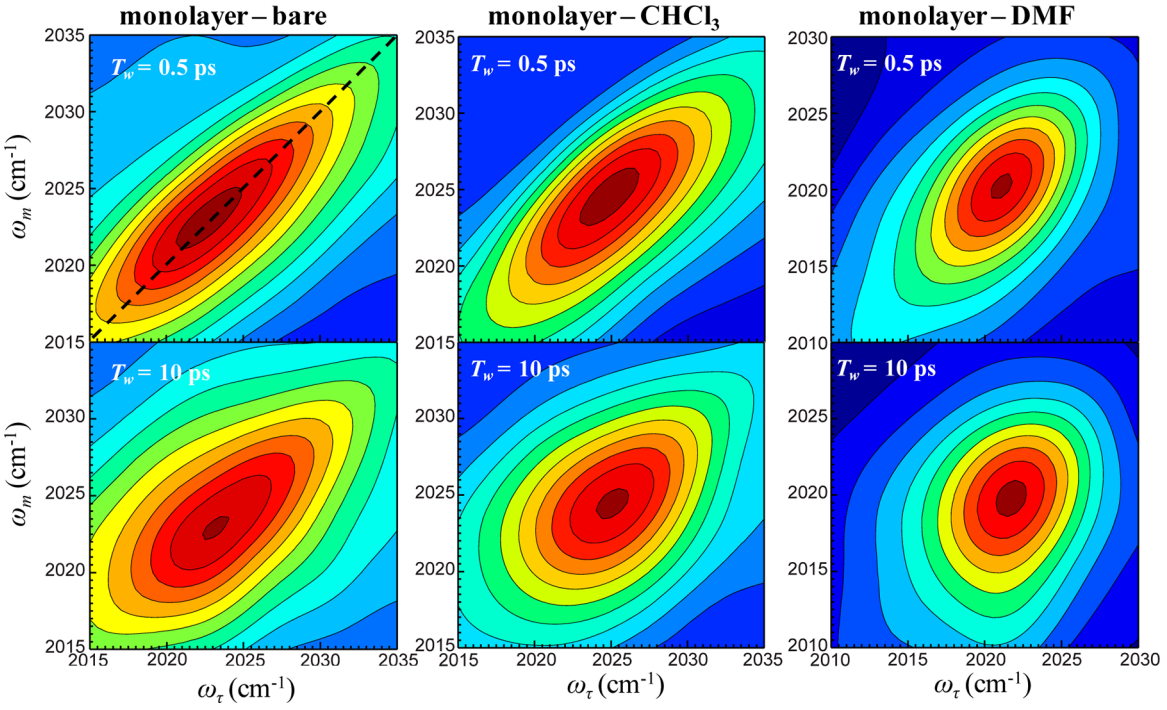

Figure 3. 2D IR spectra of the symmetric CO stretch of $RePhen(CO)_3Cl$ functionalized molecular monolayers in the absence of solvent, immersed in $CHCl_3$ and immersed in DMF. Two T_ws are shown: T_w = 0.5 ps and T_w = 10 ps.

dx.doi.org/10.1021/jp311144b | J. Phys. Chem. C 2013, 117, 1409−1420

B. 2D IR Spectroscopy and Solvent-Dependent Structural Dynamics. To understand the differences between the impact of the solvent on bulk and surface line broadening and dynamics, 2D IR spectroscopy was performed on both the $RePhen(CO)_3Cl$ headgroup in bulk solution and on functionalized monolayers immersed in liquid. The 2D IR studies of the Re complex in bulk solutions are in the solvents $CHCl_3$, DMF, THF, and MeCN. Because the headgroup is completely insoluble in hexadecane and water, the studies with hexadecane and D_2O were limited to the immersed surface.

To illustrate the nature of the data, 2D IR vibrational echo spectra of a $RePhen(CO)_3Cl$ functionalized monolayer under $CHCl_3$, DMF, and bare conditions are shown in Figure 3 at two waiting times. Changes are clearly visible in the spectra. In the early time spectra (T_w = 0.5 ps) the bare spectrum is more elongated along the diagonal (black dashed line) than either of the solvent immersed spectra, showing that the symmetric CO stretch in the bare sample is more inhomogeneously broadened with a smaller homogeneous component than the stretch in the solvent-immersed samples. Spectral diffusion occurs in all three samples as shown by the change in shape of the spectra at 10 ps compared to 0.5 ps. In DMF, spectral diffusion is extensive as shown by the large change in shape. Other solvents used (THF, MeCN) show similar spectra. The spectra for the THF immersed wafer are similar to those of $CHCl_3$, and the spectra for the MeCN immersed wafer lie in between the spectra of $CHCl_3$ and DMF in terms of spectral diffusion rate and homogeneous broadening. The 2D IR spectra of bulk solution samples have similar appearances. The bulk solution samples give much larger signals than the surface samples because of the greatly increased path length and absorbance, which results in much less noise in the determinations of the CLS. The echo signals from the surface monolayer samples have electric fields, E_{sig}, which are 50−100 times smaller than those of the bulk solution samples.

i. 2D IR Spectroscopy of the RePhen(CO)$_3$Cl Headgroup in Bulk Solution. In bulk solution of the $RePhen(CO)_3Cl$ headgroup, the symmetric CO stretch has a significant homogeneous component, and spectral diffusion occurs on the 5−10 ps time scale. Quantitative analysis of the 2D IR spectra as a function of T_w was performed using the CLS method discussed above.[56,57] The CLS is the normalized FFCF and therefore measures the remaining inhomogeneity in the absorption line after the waiting time, T_w. The CLS for the symmetric stretch of $RePhen(CO)_3Cl$ in $CHCl_3$, THF, DMF, and MeCN are plotted as a function of T_w in Figure 4. Also shown is the CLS for the symmetric CO stretch of $RePhen(CO)_3Cl$ attached to undecane by a triazole linker dissolved in $CHCl_3$ (labeled $CHCl_3$*). Much of spectral diffusion in bulk solution can be related to the reorganization of the first and to some extent the second solvent shells.[63,64] Therefore, the differences in the spectral diffusion dynamics in the bulk are representative of the different dynamics of each solvent due to their different physical and chemical properties (molecular shape, viscosity, intermolecular interactions, etc.).

From inspection of Figure 4, several observations can be made. First, the nature of the spectral diffusion is solvent dependent. The spectral diffusion occurs on multiple time scales in each solvent. The spectral diffusion in DMF and THF is biexponential, and in $CHCl_3$ it is triexponential. There are both fast and slow components to the spectral diffusion, indicating that multiple types of solvent fluctuations contribute to the spectral diffusion process. Fast processes may be

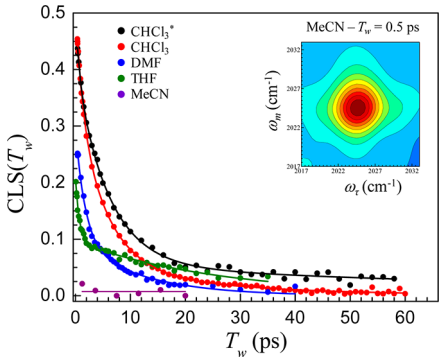

Figure 4. CLS decay curves measured for the symmetric CO stretch of $RePhen(CO)_3Cl$ in the polar organic solvents, $CHCl_3$ (red), DMF (blue), THF (green), and MeCN (purple). Also measured is the CLS decay of the $RePhen(CO)_3Cl$ headgroup covalently attached to a triazole linker on an undecane alkane chain (black; $CHCl_3$*). In MeCN there is no inhomogeneous broadening, and the line is completely homogenously broadened, as indicated by the horizontal essentially zero amplitude CLS. Parameters from the fits are reported in Table 2. The inset shows the 2D IR spectrum of the symmetric CO stretch of $RePhen(CO)_3Cl$ dissolved in MeCN at T_w = 0.5 ps. The "star" shape indicates that the absorption is homogeneously broadened.

intrasolvation shell motions, whereas slow processes may be exchange of solvent molecules between the first and second solvation shell.[63,64] The rate at which the fast and slow spectral diffusion processes occur and their relative amplitudes is highly solvent dependent.

The symmetric CO absorption line in MeCN is very different from all other samples. While all of the Re complex/solvent systems show that there is a significant homogeneous component in the absorption line by the offset from 1 in Figure 4 (see below and Table 2), MeCN is homogeneously broadened. In Figure 4, the CLS data for the MeCN solvent are a horizontal line that is at zero with no T_w dependence within experimental error. The inset in Figure 4 shows the 2D IR spectrum of the complex in MeCN at 0.5 ps. The "star" shape is characteristic of a homogeneously broadened line.[65] Since the line is homogeneously broadened, there is no inhomogeneous component and, therefore, no spectral diffusion. The fact that the line is homogeneously broadened may be due to the low viscosity, small molecular volume, and simple linear shape of MeCN, which could result in the solvent shell motions occurring on ultrafast time scales that result in no inhomogeneous broadening.

The FFCF parameters obtained from the 2D IR spectra and the CLS analysis are given in Table 2. In the multiexponential model for the FFCF given in eq 1, one of the exponentials has $\Delta\tau < 1$ and represents the motionally narrowed component. The other terms reflect the time scales (τ_i) and amplitudes (Δ_i) of the spectral diffusion (structural dynamics). As discussed above, the MeCN solvent results in a homogeneously broadened line with line width (fwhm) Γ_h = 6.1 cm^{-1}, and there are no spectral diffusion components. The CLS decays for the complex in DMF and THF are fit very well with biexponentials. As can be seen from Figure 4 and quantified in Table 2, the spectral diffusion dynamics are quite different. In comparison to the results in DMF, the THF results have a fast short time component and a slower long time component. The intermolecular interactions of the solvent with the complex produce the inhomogeneous broadening of the absorption line.

dx.doi.org/10.1021/jp311144b | J. Phys. Chem. C 2013, 117, 1409−1420

Table 2. Parameters for the FFCF for the RePhen(CO)$_3$Cl Headgroup Dissolved in Bulk Solvent[a]

solvent	Γ_h (cm^{-1})	Δ_1 (cm^{-1})	τ_1 (ps)	Δ_2 (cm^{-1})	τ_2 (ps)	Δ_3 (cm^{-1})	τ_3 (ps)	Δ_{inh} (cm^{-1})
MeCN	4.94							
DMF	3.95	1.88	1.75 ± 0.15	1.3	11.9 ± 1.3			2.29
THF	4.00	1.37	0.7 ± 0.05	1.2	26 ± 1.3			1.85
$CHCl_3$	2.67	2.03	1.2 ± 0.1	2.5	5.4 ± 0.4	0.55	25 ± 3	3.22
$CHCl_3$[b]	2.97	1.35	0.7 ± 0.25	2.57	5.95 ± 0.4	0.96	94 ± 31	3.06

[a]Γ_h = homogeneous line width (fwhm) Δ_i = amplitude of the ith spectral diffusion component (standard deviation) of the FFCF (for fwhm, multiply by 2.35), τ_i = spectral diffusion decay time for the ith component, and Δ_{inh} = total inhomogeneous line width standard deviation which is the root-mean-square of Δ_1, Δ_2, and Δ_3 (for fwhm, multiply by 2.35). Error bars are SE estimates from the fits (1σ). To calculate the total line width (observed in the FT-IR), a Lorentzian with the homogeneous line width must be convolved with a Gaussian with the total inhomogeneous line width. [b]Chromophore has triazole and alkane chain attached.

The differences in the spectral diffusion time constants in the two solvents reflect the variations in the solvent dynamical interactions with the Re complex.

The RePhen(CO)$_3$Cl in $CHCl_3$ requires a triexponential fit to reproduce the data (see Table 2). When the triazole/alkyl chain is added to the complex, the spectral diffusion in $CHCl_3$ is substantially different as is evident from the data in Figure 4. When the CLS data for the metal−carbonyl complex−triazole/alkyl chain is fit to a triexponential, the following parameters are obtained: τ_1 = 0.7 ± 0.25 ps, τ_2 = 5.95 ± 0.4 ps, and τ_3 = 94 ± 31 ps. The two fastest components decay with almost the same time constants as for the Re complex without the triazole/alkyl chain. These fluctuations are local solvent shell fluctuations. It is probable that the fast time scale decay is due to very local intrafirst-solvation shell fluctuations around the Re complex headgroup. The intermediate time scale is most likely longer time scale fluctuations of the first solvation shell. That these two components are not impacted by the presence of a triazole/alkyl chain attachment is not surprising, as these components are most likely indicative of solvent fluctuations local to the headgroup region. The slowest component in the FFCF is slowed significantly from 25 to ∼100 ps. The slowest component may be due to slow fluctuations in the extended solvation structure of the complex, which is impacted by the presence of the triazole/alkyl chain. The solvent could take longer to reorganize around the modified Re complex as it is nearly 2 times bigger than the unmodified complex. Despite the longer duration of the slowest time scale of spectral diffusion for the triazole/alkyl chain modified headgroup, the spectral diffusion dynamics with and without the triazole/alkyl chain are remarkably similar. This will be contrasted with the spectral diffusion time scale of the surface immobilized RePhen(CO)$_3$Cl headgroups exposed to solvent, which do not display fast dynamics. The slower surface dynamics cannot be attributed to the presence of the triazole/alkyl chain, as modification with the triazole/alkyl chain does not eliminate the fast spectral diffusion dynamics.

ii. Functionalized Monolayers Immersed in Headgroup Soluble Polar Organic Solvents. 2D IR spectroscopy was used to characterize RePhen(CO)$_3$Cl-functionalized molecular monolayers immersed in polar organic solvents in which the headgroup itself is soluble in bulk solution. The RePhen(CO)$_3$Cl headgroup is only soluble in polar organic solvents. The surfaces therefore can be compared to the bulk headgroup data to illustrate the differences between dynamics of molecules tethered to a surface and immersed in solvent and the dynamics in the bulk solution.

The first important question deals with the nature of the dynamics reported by the 2D IR data of the functionalized surface immersed in a solvent. Is the Re headgroup bound to the surface simply seeing the same solvent dynamics as the Re complex in bulk solutions? Figure 5 shows the CLS data for the

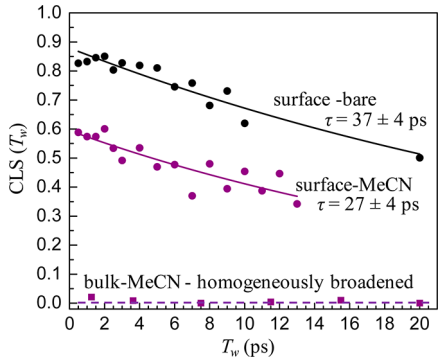

Figure 5. Experimental CLS decay curves for the symmetric CO stretch of the surface bound RePhen(CO)$_3$Cl in the absence of solvent (bare; black) and the presence of MeCN (purple dots). When immersed in MeCN, the symmetric CO stretch has a larger homogeneously component and undergoes faster spectral diffusion. Also shown is the CLS decay curve for the symmetric CO stretch of the RePhen(CO)$_3$Cl headgroup in bulk MeCN, which shows no spectral diffusion (complete homogeneous broadening). There is a clear difference between the spectral diffusion dynamics of the monolayer and in bulk solution.

surface bound complex with no solvent (bare), the surface bound complex in MeCN, and the complex in bulk MeCN. As shown in the figure, the RePhen(CO)$_3$Cl-functionalized monolayer in MeCN (purple circles) has a larger homogeneous component (larger difference from 1 at T_w = 0) than the bare sample (black circles) and decays about 40% faster. However, the contrast between the surface bound complex in MeCN and the Re headgroup in bulk MeCN is dramatic. The spectrum of the headgroup in bulk MeCN is completely homogeneously broadened, and therefore there is no spectral diffusion. Thus, the surface dynamics reported by the 2D IR experiment are not those of the solvent, but rather those of the system of surface bound chains and complexes interacting with the solvent. Although the surface dynamics are influenced by the solvent, as shown by the difference between the bare sample and the sample in MeCN, they are not simply the dynamics of the solvent. It is clear from the MeCN results that the surface inhomogeneous broadening of the absorption spectrum that is sampled by spectral diffusion is a result of chain configurations solvent interacting with the surface and not bulk solvent configurations.

dx.doi.org/10.1021/jp311144b | J. Phys. Chem. C 2013, 117, 1409−1420

The CLS data are shown for the symmetric CO stretch for solvent immersed functionalized monolayers as well as the bare sample in Figure 6. The FFCF parameters obtained from the

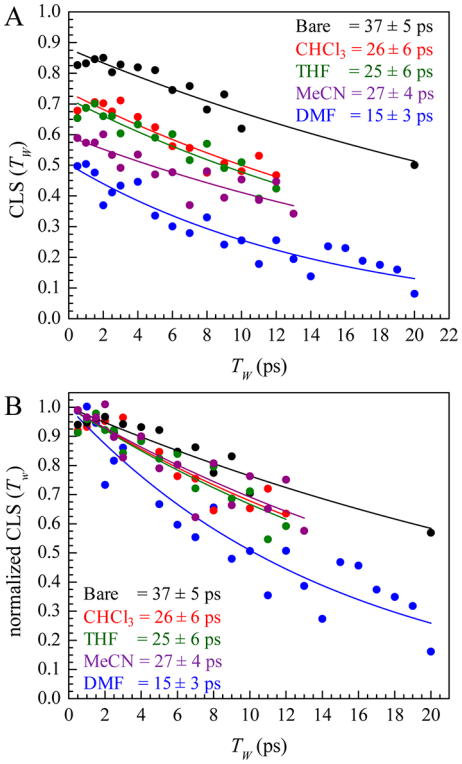

Figure 6. (A) Experimental CLS decay curves for the bare monolayer (black) and the monolayer when immersed in $CHCl_3$ (red), THF (green), MeCN (purple), and DMF (blue). (B) Normalized CLS curves for the same data as in panel A. The normalized curves illustrate that the time scales of spectral diffusion (surface dynamics) depend on the solvent.

CLS analysis and the linear absorption spectrum are given in Table 3. Figure 6A shows the experimentally measured CLS and fits. To illustrate the different time scales of spectral diffusion with different solvents, the data are also normalized by dividing by the $T_w = 0$ amplitudes of the fits and plotted again in Figure 6B. In the presence of polar organic solvents, the homogeneous component relative to the total line width increases compared to the bare sample as can be seen from the offsets from 1 in Figure 6A.[56] For the bare monolayer, the symmetric CO stretch is about 15% homogeneously broadened, whereas in the presence of organic solvent the homogeneous component accounts for between 30 and 50% of the total line width.

Table 3. Parameters for the FFCF for the RePhen$(CO)_3$Cl-Functionalized Monolayer Immersed in Solvent[a]

solvent	Γ_h (cm^{-1})	Δ (cm^{-1})	τ (ps)
bare (no solvent)	1.8	6.50	37 ± 4
headgroup soluble			
MeCN	3.2	3.82	27 ± 4
DMF	4.2	3.69	15 ± 3
THF	2.2	4.25	25 ± 6
$CHCl_3$	2.4	4.71	26 ± 6
headgroup insoluble			
hexadecane	1.9	5.27	77 ± 15
D_2O (low frequency)	2.7	5.10	46 ± 6
D_2O (high frequency)	2.8	3.74	31 ± 7

[a] Γ_h = homogeneous line width (fwhm) τ = spectral diffusion decay time, and Δ = amplitude of the spectral diffusion component (standard deviation) of the FFCF (for fwhm, multiply by 2.35). The model parameters are expressed in terms of the fwhm of the homogeneous component and the standard deviation of the inhomogeneous component.

Quantitative determinations of the homogeneous and inhomogeneous line widths of the absorption line are reported in Table 3 (the inhomogeneous line width is reported as a standard deviation; to recover the fwhm from the table multiply by 2.35). Both the homogeneous and inhomogeneous line widths are impacted by the presence and nature of the solvent. THF and $CHCl_3$ immersed samples have similar homogeneous and inhomogeneous linewidths (fwhm), 2.2 and 10.0 cm^{-1} vs 2.4 and 11.1 cm^{-1}, respectively. In MeCN, the homogeneous width is somewhat larger and the inhomogeneous width is somewhat narrower. The samples immersed in THF, $CHCl_3$, and MeCN all have very similar spectral diffusion time constants (~25 ps), as is evident from Figure 6B, where the lines reflecting the fits to the data for the three solvents (red, green, and purple lines) are virtually the same. This is contrasted to the DMF immersed sample, which has a larger homogeneous line width (4.2 cm^{-1}) and a narrower inhomogeneous line width (fwhm = 8.7 cm^{-1}). MeCN lies between THF/$CHCl_3$ and DMF in terms of changes to the homogeneous and inhomogeneous broadening (3.2 and 9.0 cm^{-1}).

The inhomogeneous line width can vary in the presence of different solvents through changes in the microstructure of the monolayer, which can change the distribution of vibrational frequencies. Changes in the microstructure may involve some penetration of the solvent into the monolayer as well as the influence of surface interfacial solvent layer. In all of the polar organic solvents for which the headgroup is soluble in bulk solution, the spectral diffusion is faster than that observed for the bare sample (see Figure 6B and Table 3). The rate of spectral diffusion is a measure of the structural evolution of the system. As discussed above in connection with Figure 6, the spectral diffusion measured for the functionalized surfaces immersed in solvent is observing the surface dynamics rather than only measuring the bulk solvent dynamics. That the measurements on the surface samples reflect surface dynamics is further reinforced by the differences from the bulk measurements for all of the bulk solution samples (see Figure 4 and Table 2). The bare spectral diffusion time is nearly identical to the one measured for five different RePhen-$(CO)_3$Cl-functionalized monolayers in our previous work.[10]

Other than DMF (15 ps), the polar organic solvents all have essentially identical time scales of spectral diffusion (~25 ps) regardless of viscosity, molecular volume, or molecular structure of the solvent molecule. $CHCl_3$, THF, and MeCN have different chemical interactions with the surface. $CHCl_3$ can interact through the partial positive charge of the proton, or the large polarizable electron clouds of the chlorines, whereas THF can interact through CH, ether, or dipole interactions. MeCN can interact through strong dipolar interactions, and CN is a good ligand for Re. The chemical differences are clearly visible through the surface IR absorption spectra, which show that for the surface immersed in solvents, the symmetric CO stretch has a different shift from the bare sample absorption.

dx.doi.org/10.1021/jp311144b | J. Phys. Chem. C 2013, 117, 1409−1420

Table 4. Vibrational Relaxation Parameters for the Symmetric CO Stretch of RePhen(CO)$_3$Cl-Functionalized Monolayers and the RePhen(CO)$_3$Cl Headgroup in the Bulk[a]

solvent	A_1	τ_1^r (ps)	A_2	τ_2^r (ps)	A_{1bulk}	τ_{1bulk}^r (ps)	A_{2bulk}	τ_{2bulk}^r (ps)
bare	0.23 ± 0.04	1.75 ± 0.4	0.77 ± 0.2	21 ± 0.3				
MeCN			1	20 ± 0.3	0.19	1.18 ± 0.04	0.81	27.02 ± 0.05
DMF			1	17 ± 0.3	0.20	1.52 ± 0.03	0.80	22.00 ± 0.03
THF			1	18.5 ± 0.3	0.21	1.53 ± 0.06	0.879	28.14 ± 0.08
$CHCl_3$	0.35 ± 0.02	1.67 ± 0.2	0.65 ± 0.04	31 ± 0.2	0.20	2.12 ± 0.06	0.80	41.48 ± 0.09
D_2O			1	20 ± 2				
$C_{16}H_{34}$			1	18.8 ± 0.3				

[a] A_i = amplitude of the ith component in the vibrational relaxation model. First four columns: surface; second four columns: headgroup in bulk solution when soluble. τ_i^r = decay times for vibrational relaxation. The HDTG signal decays are fit to biexponential models, $H(T_w) = A_1 \exp(-T_w/\tau_1^r) + A_2 \exp(-T_w/\tau_2^r)$, where $\tau_2^r > \tau_1^r$. For single-exponential decays, the decay constant is reported as τ_2^r. The total amplitudes are normalized to 1. Error bars are SE of parameter (1σ). SEs of the bulk amplitudes are <0.01.

Despite the differences between the headgroup−solvent interaction, the spectral diffusion times are similar, again showing that the solvent changes the structural dynamics of the monolayer. The solvent impacts these dynamics through chemical interaction with the monolayer, but the dynamics do not change in a simple fashion that is predictable from the bulk.

The faster structural evolution (spectral diffusion) of the functionalized monolayer immersed in DMF may be indicative of differences in the structure compared to the effects other polar organic solvents. It is possible that DMF has strong interactions with the headgroup as DMF is the best bulk solvent studied for the RePhen(CO)$_3$Cl headgroup with a saturation concentration of 28 mM vs 1.1 mM (THF), 1.6 mM ($CHCl_3$), and 1.9 mM (MeCN). The solubility data suggest that DMF has stronger interactions with the RePhen(CO)$_3$Cl headgroup that result in a more negative enthalpy of solvation. The strong headgroup−DMF interactions may modify the surface structure since RePhen(CO)$_3$Cl is a significant volume fraction of the total organic layer deposited on silica. Differences in structure will result in changes in dynamics of the monolayer. The influence of the solvent on the structure and therefore the dynamics is amplified by the results presented in the next section.

The homogeneous line width is usually primarily determined by the motionally narrowed pure dephasing contribution to the absorption line. However, there are also contributions to the homogeneous line width from vibrational relaxation and molecular reorientation. Orientational relaxation for the bare sample was measured using polarized HDTG experiments. There is orientational relaxation on a ∼1 ps time scale, but it has a very small amplitude, which was attributed to a small degree of orientational wobbling-in-a-cone.[10] The small extent of the orientational relaxation will result in a negligible contribution to the homogeneous line width, as the orientational correlation function is nearly static except for a small drop in the first few picoseconds. It is likely that the orientational relaxation when the surface is immersed in solvents is also severely constrained by the chain packing and therefore makes a very small contribution to the homogeneous line width.

The lifetime contribution to the homogeneous line width is uncertain. The population decays of all the bulk samples were measured with pump−probe experiments (transient absorption) at the magic angle probe polarization relative to the pump-polarization. Probing at the magic angle eliminates orientational relaxation contributions to the transient absorption decays.[66,67] Therefore, the measured decays are strictly due to population relaxation. For the surface samples HDTG spectroscopy was performed with parallel polarization, as the depolarization due to reorientation was found to be small and does not significantly impact the HDTG decay.[10] The measurement for the surfaces are therefore nearly completely indicative of population decay. The results for the surface samples and for the bulk Re complex headgroup are given in Table 4. All of the bulk solution samples and several of the surface samples display biexponential decays (see Table 4). The slow component is found to be lengthened by the presence of chloroform in the bulk and at the surface. The frequency shift and extension of the lifetime are consistent with the role of π^* back-bonding in the vibrational structure and dynamics of CO ligands.[68,69] The slow component is far too slow to make a significant contribution to the homogeneous line width. A 20 ps decay will contribute ∼0.25 cm^{-1} to the homogeneous line width. However, the fast component almost certainly arises from relaxation from the initially pumped higher frequency symmetric carbonyl stretch into the two lower frequency carbonyl stretching modes. This relaxation does not impact the spectral diffusion, but it can produce a significant contribution to the homogeneous line width. Since there are two lower frequency vibrational levels, it is possible that there is a fast relaxation rate that is too fast to observe with the pulse duration used in the experiments. To investigate this possibility, experiments would have to be conducted with much shorter pulses, and therefore larger bandwidths such that all three carbonyl stretching modes are within the laser bandwidth. By observing all three modes in 2D IR and pump−probe experiments, it is possible to determine the relaxation rates among the modes. While vibrational relaxation among modes of a molecule is an interesting problem, it is not important for the issues of interest here. Again, it is important to emphasize that fast relaxation into the lower frequency modes can contribute to the homogeneous line width but does not influence the measurement of spectral diffusion.

iii. Functionalized Monolayers Immersed in Headgroup Insoluble Solvents. 2D IR spectroscopy was performed on the same monolayers immersed in hexadecane and D_2O, solvents in which the headgroup RePhen(CO)$_3$Cl is completely insoluble. These liquids are in contrast to the polar organic solvents discussed above in which the Re complex headgroup is soluble. Figure 7 shows the data for the functionalized surface immersed in hexadecane and the bare surface for comparison. As can be seen from the CLS plot, the spectral diffusion of the surface monolayer (77 ± 15 ps) is very slow, slower even than

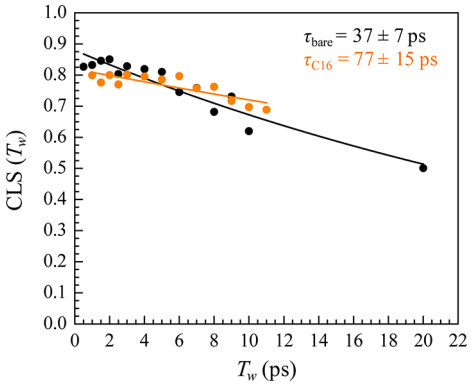

Figure 7. Experimental CLS decay curves for the symmetric CO stretch of immobilized RePhen(CO)$_3$Cl in the absence of solvent (bare; black) and in the presence of hexadecane (orange). The spectral diffusion process with the surface in contact with hexadecane (headgroup insoluble) is slowed compared to the bare surface in contrast to the acceleration in polar organic solvents (headgroup soluble).

the bare surface (33 ± 7 ps). The FFCF parameters are given in Table 3. The slow decay when the surface is immersed in hexadecane is in contrast to the samples in the polar organic solvents in which the spectral diffusion of the surface layer is faster than the bare surface in all of the solvents (see Table 3).

Figure 2 shows the FT-IR absorption spectrum of the symmetric CO stretch of the Re complex functionalized surface immersed in D_2O. D_2O is used to mitigate the strong absorption by the solvent that occurs even when a submicrometer layer of H_2O is used. The spectrum is composed of two absorption lines, which demonstrates that there are two distinct environments for the Re complex headgroup. Although the 2D IR bands overlap, CLS analysis can be performed on each band individually by selecting the correct region of the spectrum to examine.[70] The CLS decays for the two bands are shown in Figure 8 and yield decay times

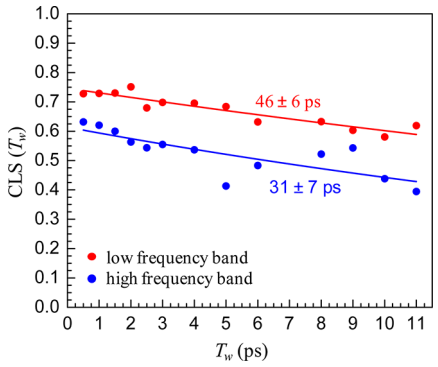

Figure 8. CLS points measured for the RePhen(CO)$_3$Cl monolayer immersed in D_2O. The CLS points are calculated for the red side (2020−2025 cm^{-1}, red) and the blue side (2032−2036 cm^{-1}, blue) independently.

of 46 ± 6 ps (low-frequency band in Figure 2) and 31 ± 7 (high-frequency band in Figure 2). The FFCF parameters are given in Table 3. The FT-IR spectrum in Figure 2 shows that there are two environments in the surface layer for the Re complex headgroups. The 2D IR results show that these environments have different structural dynamics. The major site is the low-frequency site as can be seen from the spectrum in Figure 2. The dynamics of molecules in the environment that gives rise to the low-frequency band are slightly slower than those of the bare surface (see Table 3). Like hexadecane, when the surface is immersed in a solvent in which the Re complex is not soluble in bulk solution, the dynamics are slower than that of the dry surface. However, the dynamics of the minor site (high-frequency band in Figure 2) are somewhat faster than those of the bare surface, although the error bars overlap. Nonetheless, the minor site has dynamics that are still slower than those of the surface immersed in any of the polar organic solvent in which the Re complex is soluble in bulk solution. The spectral diffusion of the major site has been replicated on a second wafer and measured to be 41 ± 5 ps, again slightly slower than the bare surface, consistent with the first wafer measurements. The minor site peak amplitude is sample dependent, and although the FT-IR spectrum showed the presence of a second absorption band, the amplitude was too low to extract a CLS curve from the 2D spectra.

When the surface is immersed in hexadecane and D_2O, liquids that do not dissolve the Re complex in bulk solution, the dynamics are slower than they are when the surface is immersed in polar organic solvents that do dissolve the headgroup in bulk solutions. The difference in the dynamics suggests that there is a significant change in the surface structure in the two types of solvents. The polar organic liquids may swell the surface layer to some extent with solvent penetration into the layer while the other liquids may repel the headgroups causing a compaction of the surface. Such a difference would result in distinct dynamics and might also affect the catalytic activity of a heterogeneous catalyst.

IV. CONCLUDING REMARKS

The structural dynamics of functionalized monolayers immersed in liquids, as reported on by the spectral diffusion of the symmetric CO stretch of RePhen(CO)$_3$Cl measured with 2D IR vibrational echo experiments, are different from the bare surface (surface in air). The dynamics differ depending on the liquid, and there is a particular distinction between polar organic liquids that dissolve the Re complex in bulk solution (DMF, $CHCl_3$, THF, and acetonitrile) and liquids in which the headgroup is insoluble (hexadecane and D_2O). The 2D IR experiments were also conducted on the Re complex in the bulk liquids in which it is soluble. There are significant differences between the dynamics observed for the surface bound complex and those for the complex in bulk solution. This is shown clearly in Figure 5 for acetonitrile. The detailed results of the 2D IR experiments, in terms of the frequency−frequency correlation function parameters, are given in Table 3.

Spectral diffusion in the bulk is driven by changes in the solvation structure;[63,64] spectral diffusion at the surface is dominated by interactions of the tethered molecules with the monolayer itself and solvent molecules immediately in contact with it. Different solvents impact these two situations (bulk vs surface) differently, and the differences are apparent in the picosecond time scale dynamics. DMF causes the structural dynamics of the monolayer to accelerate beyond that of any other solvents studied.

The Re complex is not soluble in bulk hexadecane. When the functionalized surface is immersed in hexadecane, the resulting spectral diffusion is the slowest that is observed for any of the solvents studied to date (see Figure 7 and Table 3). The spectral diffusion in hexadecane is even slower than that of the bare functionalized surface. The results suggest that the surface

dx.doi.org/10.1021/jp311144b | J. Phys. Chem. C 2013, 117, 1409−1420

structure is quite different in a liquid in which the headgroup is not soluble than in a headgroup soluble liquid. The headgroup insoluble liquids may compact the surface monolayer, resulting in a more restrictive structure and slower dynamics.

The manner in which water influences the structure and dynamics of hydrophobic surfaces is an important question in the study of the physical chemistry of surfaces, which we have begun to address. The CO symmetric stretch IR absorption spectrum of $RePhen(CO)_3Cl$ monolayers when immersed in D_2O shows two sites (see Figure 2) and slower spectral diffusion than organic solvents. The major site has dynamics that are slower than the bare surface, like hexadecane. The two sites display different spectral diffusion time scales, which indicates the structures of these two sites undergo different rates of structural evolution. These results show that water has an impact on the hydrophobic monolayer dynamics, despite the fact that the monolayer is hydrophobic.

AUTHOR INFORMATION

Corresponding Author

*E-mail fayer@stanford.edu.

Notes

The authors declare no competing financial interest.

ACKNOWLEDGMENTS

This material is based upon work supported by the Air Force Office of Scientific Research Grant FA9550-12-1-0050 which supported the surface experiments and chemistry. This work was also funded by the Division of Chemical Sciences, Geosciences, and Biosciences, Office of Basic Energy Sciences of the U.S. Department of Energy through Grant DE-FG03-84ER13251, which made contributions to the 2D IR measurements in solution. Daniel E. Rosenfeld also thanks the Fannie and John Hertz Foundation, the National Science Foundation, and the Stanford Graduate Fellowship programs for graduate fellowships.

REFERENCES

(1) Baker, M. A.; Li, J. *Surf. Interface Anal.* **2006**, *38*, 863−867.
(2) Gooding, J. J.; Mearns, F.; Yang, W.; Liu, J. *Electroanalysis* **2003**, *15*, 81−96.
(3) Walter, S. R.; Youn, J.; Emery, J. D.; Kewalramani, S.; Hennek, J. W.; Bedzyk, M. J.; Facchetti, A.; Marks, T. J.; Geiger, F. M. *J. Am. Chem. Soc.* **2012**, *134*, 11726−11733.
(4) Bent, S. F.; Kachian, J. S.; Rodríguez-Reyes, J. C. F.; Teplyakov, A. V. *Proc. Natl. Acad. Sci. U. S. A.* **2011**, *108*, 956−960.
(5) Somorjai, G. A.; Li, Y. *Proc. Natl. Acad. Sci. U. S. A.* **2011**, *108*, 917−917.
(6) De Vos, D. E.; Dams, M.; Sels, B. F.; Jacobs, P. A. *Chem. Rev.* **2002**, *102*, 3615−3640.
(7) Kenvin, J. C.; White, M. G.; Mitchell, M. B. *Langmuir* **1991**, *7*, 1198−1205.
(8) Bailey, D. C.; Langer, S. H. *Chem. Rev.* **1981**, *81*, 109−148.
(9) Rosenfeld, D. E.; Gengeliczki, Z.; Smith, B. J.; Stack, T. D. P.; Fayer, M. D. *Science* **2011**, *334*, 634−639.
(10) Rosenfeld, D. E.; Nishida, J.; Yan, C.; Gengeliczki, Z.; Smith, B. J.; Fayer, M. D. *J. Phys. Chem. C* **2012**, *116*, 23428−23440.
(11) Nicodemus, R. A.; Ramasesha, K.; Roberts, S. T.; Tokmakoff, A. *J. Phys. Chem. Lett.* **2010**, *1*, 1068−1072.
(12) Ramasesha, K.; Roberts, S. T.; Nicodemus, R. A.; Mandal, A.; Tokmakoff, A. *J. Chem. Phys.* **2011**, *135*, 054509.
(13) Roberts, S. T.; Ramasesha, K.; Tokmakoff, A. *Acc. Chem. Res.* **2009**, *42*, 1239−1249.
(14) Asbury, J. B.; Steinel, T.; Kwak, K.; Corcelli, S. A.; Lawrence, C. P.; Skinner, J. L.; Fayer, M. D. *J. Chem. Phys.* **2004**, *121*, 12431−12446.
(15) Asbury, J. B.; Steinel, T.; Stromberg, C.; Gaffney, K. J.; Piletic, I. R.; Goun, A.; Fayer, M. D. *Chem. Phys. Lett.* **2003**, *374*, 362−371.
(16) Fayer, M. D.; Moilanen, D. E.; Wong, D.; Rosenfeld, D. E.; Fenn, E. E.; Park, S. *Acc. Chem. Res.* **2009**, *42*, 1210−1219.
(17) Zheng, J.; Kwak, K.; Fayer, M. D. *Acc. Chem. Res.* **2006**, *40*, 75−83.
(18) Kim, Y. S.; Hochstrasser, R. M. *Proc. Natl. Acad. Sci. U. S. A.* **2005**, *102*, 11185−11190.
(19) Backus, E. H. G.; Bloem, R.; Donaldson, P. M.; Ihalainen, J. A.; Pfister, R.; Paoli, B.; Caflisch, A.; Hamm, P. *J. Phys. Chem. B* **2010**, *114*, 3735−3740.
(20) Bredenbeck, J.; Helbing, J.; Nienhaus, K.; Nienhaus, G. U.; Hamm, P. *Proc. Natl. Acad. Sci. U. S. A.* **2007**, *104*, 14243−14248.
(21) Middleton, C. T.; Marek, P.; Cao, P.; Chiu, C.-c.; Singh, S.; Woys, A. M.; de Pablo, J. J.; Raleigh, D. P.; Zanni, M. T. *Nat. Chem.* **2012**, *4*, 355−360.
(22) Moran, S. D.; Woys, A. M.; Buchanan, L. E.; Bixby, E.; Decatur, S. M.; Zanni, M. T. *Proc. Natl. Acad. Sci. U. S. A.* **2012**, *109*, 3329−3334.
(23) Falvo, C.; Zhuang, W.; Kim, Y. S.; Axelsen, P. H.; Hochstrasser, R. M.; Mukamel, S. *J. Phys. Chem. B* **2012**, *116*, 3322−3330.
(24) Fang, C.; Hochstrasser, R. M. *J. Phys. Chem. B* **2005**, *109*, 18652−18663.
(25) Dutta, S.; Rock, W.; Cook, R. J.; Kohen, A.; Cheatum, C. M. *J. Chem. Phys.* **2011**, *135*, 055106.
(26) Bredenbeck, J.; Helbing, J.; Behrendt, R.; Renner, C.; Moroder, L.; Wachtveitl, J.; Hamm, P. *J. Phys. Chem. B* **2003**, *107*, 8654−8660.
(27) Thielges, M. C.; Chung, J. K.; Fayer, M. D. *J. Am. Chem. Soc.* **2011**, *133*, 3995−4004.
(28) Thielges, M. C.; Fayer, M. D. *Acc. Chem. Res.* **2012**, *45*, 1866−1874.
(29) Mukherjee, P.; Kass, I.; Arkin, I. T.; Zanni, M. T. *Proc. Natl. Acad. Sci. U. S. A.* **2006**, *103*, 3528−3533.
(30) Singh, P. C.; Nihonyanagi, S.; Yamaguchi, S.; Tahara, T. *J. Chem. Phys.* **2012**, *137*, 094706−094706.
(31) Xiong, W.; Laaser, J. E.; Mehlenbacher, R. D.; Zanni, M. T. *Proc. Natl. Acad. Sci. U. S. A.* **2011**, *108*, 20902−20907.
(32) Zhang, Z.; Piatkowski, L.; Bakker, H. J.; Bonn, M. *Nat. Chem.* **2011**, *3*, 888−893.
(33) Bredenbeck, J.; Ghosh, A.; Nienhuys, H. K.; Bonn, M. *Acc. Chem. Res.* **2009**, *42*, 1332−1342.
(34) Bredenbeck, J.; Ghosh, A.; Smits, M.; Bonn, M. *J. Am. Chem. Soc.* **2008**, *130*, 2152−2153.
(35) Nihonyanagi, S.; Singh, P.; Yamaguchi, S.; Tahara, T. *Bull. Chem. Soc. Jpn.* **2012**, *85*, 758−760.
(36) McGuire, J. A.; Shen, Y. R. *Science* **2006**, *313*, 1945−1948.
(37) Shen, Y. R.; Ostroverkhov, V. *Chem. Rev.* **2006**, *106*, 1140−1154.
(38) Tian, C. S.; Shen, Y. R. *Proc. Natl. Acad. Sci. U. S. A.* **2009**, *106*, 15148−15153.
(39) Eftekhari-Bafrooei, A.; Borguet, E. *J. Phys. Chem. Lett.* **2011**, *2*, 1353−1358.
(40) Poynor, A.; Hong, L.; Robinson, I. K.; Granick, S.; Zhang, Z.; Fenter, P. A. *Phys. Rev. Lett.* **2006**, *97*, 266101.
(41) Scherge, M.; Li, X.; Schaefer, J. A. *Tribol. Lett.* **1999**, *6*, 215−220.
(42) Tian, F.; Xiao, X.; Loy, M. M. T.; Wang, C.; Bai, C. *Langmuir* **1998**, *15*, 244−249.
(43) Deng, K.; Collins, R. J.; Mehregany, M.; Sukenik, C. N. *J. Electrochem. Soc.* **1995**, *142*, 1278−1285.
(44) Hawecker, J.; Lehn, J.-M.; Ziessel, R. *J. Chem. Soc., Chem. Commun.* **1983**, 536−538.
(45) Hawecker, J.; Lehn, J.-M.; Ziessel, R. *Helv. Chim. Acta* **1986**, *69*, 1990−2012.
(46) Pac, C.; Ishii, K.; Yanagida, S. *Chem. Lett.* **1989**, *18*, 765−768.
(47) Kurz, P.; Probst, B.; Spingler, B.; Alberto, R. *Eur. J. Inorg. Chem.* **2006**, 2966−2974.
(48) Morris, A. J.; Meyer, G. J.; Fujita, E. *Acc. Chem. Res.* **2009**, *42*, 1983−1994.

(49) Sullivan, B. P.; Meyer, T. J. *Organometallics* **1986**, *5*, 1500−1502.
(50) Park, S.; Kwak, K.; Fayer, M. D. *Laser Phys. Lett.* **2007**, *4*, 704−718.
(51) Kumar, S. K. K.; Tamimi, A.; Fayer, M. D. *J. Chem. Phys.* **2012**, *137*, 184201.
(52) Shim, S.-H.; Zanni, M. T. *Phys. Chem. Chem. Phys.* **2009**, *11*, 748−761.
(53) Bloem, R.; Garrett-Roe, S.; Strzalka, H.; Hamm, P.; Donaldson, P. *Opt. Express* **2010**, *18*, 27067−27078.
(54) Tan, H.-S. *J. Chem. Phys.* **2008**, *129*, 124501.
(55) Middleton, C. T.; Strasfeld, D. B.; Zanni, M. T. *Opt. Express* **2009**, *17*, 14526−14533.
(56) Kwak, K.; Park, S.; Finkelstein, I. J.; Fayer, M. D. *J. Chem. Phys.* **2007**, *127*, 124503.
(57) Kwak, K.; Rosenfeld, D. E.; Fayer, M. D. *J. Chem. Phys.* **2008**, *128*, 204505.
(58) Fayer, M. D. *Annu. Rev. Phys. Chem.* **1982**, *33*, 63−87.
(59) Tokmakoff, A.; Fayer, M. D.; Banholtzer, W. *Appl. Phys. A: Mater. Sci. Process.* **1993**, *56*, 87−90.
(60) Goodno, G. D.; Dadusc, G.; Miller, R. J. D. *J. Opt. Soc. Am. B* **1998**, *15*, 1791−1794.
(61) Scodinu, A.; Fourkas, J. T. *J. Phys. Chem. B* **2002**, *106*, 10292−10295.
(62) Knox, R. S. *Photochem. Photobiol.* **2003**, *77*, 492−496.
(63) Kwak, K. W.; Park, S.; Fayer, M. D. *Proc. Natl. Acad. Sci. U. S. A.* **2007**, *104*, 14221−14226.
(64) Schweizer, K. S.; Chandler, D. *J. Chem. Phys.* **1982**, *76*, 2296−2314.
(65) Sanda, F.; Mukamel, S. *J. Chem. Phys.* **2006**, *125*, 014507−014512.
(66) Tan, H. S.; Piletic, I. R.; Fayer, M. D. *J. Opt. Soc. Am. B: Opt. Phys.* **2005**, *22*, 2009−2017.
(67) Tokmakoff, A. *J. Chem. Phys.* **1996**, *105*, 1−12.
(68) Dlott, D. D.; Fayer, M. D.; Hill, J. R.; Rella, C. W.; Suslick, K. S.; Ziegler, C. J. *J. Am. Chem. Soc.* **1996**, *118*, 7853−7854.
(69) Hill, J. R.; Ziegler, C. J.; Suslick, K. S.; Dlott, D. D.; Rella, C. W.; Fayer, M. D. *J. Phys. Chem.* **1996**, *100*, 18023−18032.
(70) Fenn, E. E.; Fayer, M. D. *J. Chem. Phys.* **2011**, *135*, 074502−074515.